Draft version June 30, 2015
Preprint typeset using LaTeX style emulateapj v. 12/16/11

Marz: MANUAL AND AUTOMATIC REDSHIFTING SOFTWARE

S. R. Hinton[1,2], T. M. Davis[1,2], C. Lidman[2,3], K. Glazebrook,[4], and G. F. Lewis[5]

Draft version June 30, 2015

ABSTRACT

The Australian Dark Energy Survey (OzDES) is a 100-night spectroscopic survey underway on the Anglo-Australian Telescope using the fibre-fed 2-degree-field (2dF) spectrograph. We have developed a new redshifting application Marz with greater usability, flexibility, and the capacity to analyse a wider range of object types than the runz software package previously used for redshifting spectra from 2dF. Marz is an open-source, client-based web-application which provides an intuitive interface and powerful automatic matching capabilities to consume FITs files generated from the AAOmega spectrograph and produce high quality spectroscopic measurements. Behind the scenes, a cross-correlation algorithm is used to match input spectra against a variety of stellar and galactic templates, and automatic matching performance for high quality spectra has increased from 57% (runz) to 94% (Marz). Spectra not matched correctly by the automatic algorithm can be easily redshifted manually by cycling automatic results, manual template comparison, or marking spectral features.

1. INTRODUCTION

The Australian arm of the Dark Energy Survey (OzDES) is a five-year, 100-night spectroscopic survey using the Anglo-Australia Telescope (AAT), and aims to provide accurate spectroscopic redshifts of Type Ia supernova hosts, photo-z targets emission line galaxies (EML) and radio galaxies between redshift ranges of $0.1 \leq z \leq 1.2$, in addition to spectroscopic measurements of active galactic nuclei and quasars in the redshift range of $0.3 \leq z \leq 4.5$ Yuan *et al.* (2015). A close collaborator with OzDES is the newly formed 2dFLenS survey [6] which aims to measure the redshift-space distortion of 985 square degrees in its 50-night spectroscopic survey using with AAT. The process of extracting redshifts from spectroscopic measurements is thus required to be robust across a wide variety of target types, and since our aim is primarily to acquire redshifts, our survey will be most efficient when we can extract redshifts from low signal-to-noise spectra.

A variety of redshifting solutions have been developed in the past, with much of the developed software being spectrograph or survey specific. runz was written for use by the 2dF galaxy redshift survey (Colless *et al.* 2001), and the OzDES team has previously relied on a version of the runz software package modified by Saunders *et al.* (2004) for use in the WiggleZ survey. It is primarily against this modified version of runz that we compare results to in this report. Unfortunately, there are several reasons why neither the runz software package, nor other available redshifting software packages, were sufficient for use in the OzDES survey. The foremost problem with using the existing software solution was the inclusion of more varied target object types at a lower signal-to-noise ratio than prior surveys, and the resulting decrease in automatic matching capacity by the legacy software created an unsustainable workload for the members of the OzDES team to manually redshift observed spectra. In addition to this, the legacy nature of the runz code base makes code updates difficult, installation and usage overly complicated for members of the team and especially difficult for new members to learn. The sum of these factors prompted the development of a modern software replacement.

It is from the above motivation that a set of minimum requirements were drawn up for the proposed software project. First and foremost, the automatic matching capacity had to exceed that of runz, and the software would have to present an intuitive interface to allow manual redshifting by the user. In regards to its basic usability, requirements were for it to be easy to install, operating system independent, and able to update itself without user prompting.

2. PLATFORM

The choice of utilising a browser platform by implementing the matching software as a web application allows access to the software from any laptop or desktop with an internet connection. The interface utilises Google's AngularJS framework and HTML5's Web Worker API for multi-threaded processing, along with Twitter's Bootstrap via Angular UI's Bootstrap components to allow for rapid UI development and prototyping with minimal code boilerplate and reimplementation of common tasks. Communication to Web Workers and any future potential server communication will use JSON format, and will conform to the REST interface. Utilisation of local storage has the benefit that results are not lost when exiting the application or refreshing the browser, negating one of the major disadvantages of stateful web applications. Settings changes are persisted

[1] Department of Physics, The University of Queensland, Brisbane, QLD 4072, Australia
[2] ARC Centre of Excellence for All-sky Astrophysics (CAASTRO)
[3] Australian Astronomical Observatory, North Ryde, NSW 2113, Australia
[4] Centre for Astrophysics and Supercomputing, Swinburne, University of Technology, Hawthorn, VIC 3122, Australia
[5] Sydney Institute for Astronomy, School of Physics, A28, The University of Sydney, NSW, 2006, Australia
[6] `http://astronomy.swin.edu.au/~cblake/2dflens_proposal.pdf`

via setting cookie properties instead of using local storage.

The code base for Marz is hosted publically on GitHub[7], allowing for open issue management, feature requests, open collaboration, forking of the project and instant web-hosting[8].

3. MATCHING ALGORITHM

The algorithm that takes an observed spectrum and measures the redshift is the heart of any redshifting program. The matching algorithms in Marz utilise a modified version of the autoz algorithm implemented by Baldry *et al.* (2014). In light of the success of χ^2 algorithms in modern surveys Bolton *et al.* (2012) an initial χ^2 algorithm was developed, but was consistently outperformed by the cross correlation algorithm and discarded. FITS file input from the AAOmega spectrograph undergo two distinct steps of processing: (1) the preprocessing stage to clean the data and (2) the matching process to align the observed spectra with template spectra, simultaneously finding the best-fit object type and shifting it to the best-fit redshift.

The preprocessing stage is designed to remove any bad pixels and cosmic rays from the data before being returned back to the interface, so that the user can manually redshift using the cleaned data.

- **Bad pixels** are defined when the intensity spectrum is not a number, negative or exceeds a certain configurable threshold, or if the variance spectrum for the pixel is negative.
- **Cosmic rays** are identified via neighbouring pixels exceeding thirty standard deviations from the mean.

Both bad pixels and cosmic rays are replaced with a mean of four and two pixels to either side respectively. Continuum is initially subtracted via the method of rejected polynomial subtraction, where a 6-degree polynomial is iteratively fitted to the spectrum and, as with autoz, all points greater than 3.5 standard deviations from the mean are removed from the fitting process. As soon as an iteration discards no extra pixels, or after fifteen iterations, the loop is terminated and the final polynomial should closely follow the continuum, and is thus subtracted out. Figure 2 illustrates each step in this process. This initial round of continuum subtraction is not intended to be high enough quality for the automatic matching process, it is done to give the user the option of manually redshifting spectra without continuum, allowing them to focus on the emission and absorption features of the spectrum without the broad shape of the continuum to distract. In order to limit the effect singular emission features can have on spectrum matching, all features are clipped at a distance of 30 standard deviations from the mean. Unlike many redshifting programs, heliocentric corrections are not applied to the spectra as they are expected to have been applied already in the given spectra. This is in light of the high amount of stacking done in the OzDES team, where spectra from different observation runs are stacked together to increase the signal-to-noise ratio. As these observations are generally on different nights and during different times in the night, each of them should have its own heliocentric correction applied before being stacked, and as such the spectra given to Marz are assumed to have come through a data pipeline which includes heliocentric correction.

The matching process, which takes the output of the preprocessing step in the form of an intensity and variance spectrum Tam, you said to define variance spectrum. What do you mean, isn't 'variance' itself the definition?, first duplicates the intensity spectrum so that two copies exist internally. This is necessary because the matching of the broad-featured quasar template differs to matching of the other templates, and the copy of the intensity spectrum used for quasar matching shall now be referred to as the quasar spectrum, and the other spectrum - used to match all other templates, shall be referred to as the general spectrum. In order to better match the smooth quasar template, the quasar spectrum undergoes smoothing via a rolling-point exponential decay mean function of window width 7 pixels, with exponential decay factor of 0.9. As the sharp features of the general templates are not benefited by smoothing, the general spectrum instead undergoes a second step of continuum subtraction, where a boxcar smoothed median filter (121 pixel window of boxcar smoothing and 51 pixel window median filter) is subtracted from the spectrum. This step is not applied to the quasar spectrum, as the fineness of the smoothed median subtraction would result in broad features being completely removed from the spectrum.

The general spectrum then has error adjustment applied, where each pixel has its variance set to the maximal value of itself and the variance of its two neighbouring pixels. Following Baldry *et al.* (2014), this is to allow for uncertainty in the sky subtraction and any underestimation of errors next to sky lines. The variance spectrum is then widened again, where each pixel is set to a maximum of its original value or 70% of a thirteen pixel median filter of width 13 pixels, which serves to remove from the variance any points of sufficiently low variance that division of the intensity by the variance would create a fake emission feature. The intensity of the general spectrum is divided by the variance spectrum to down-weight pixels with higher uncertainty. As we wish to preserve broad features found in quasar spectra, we require the quasar error spectrum to be sufficiently smooth that broad features are not destroyed when we apply the variance onto the spectr[illegible]ntensity. A median filter of 81 pixel width is applied to the variance, and then the result is smoothed with boxcar smoothing using a window of 25 pixels. In order to preserve even more broad shape by creating a more uniform variance, the variance of the spectrum is increased by addition of twenty times the minimum spectru[illegible]riance. The quasar intensity is then divided by the [illegible]sted variance to product a spectrum that retains broad features and shapes, but down weights sections of higher variance which are commonly found

[7] https://github.com/Samreay/Marz
[8] Marz can be found at http://samreay.github.io/Marz/

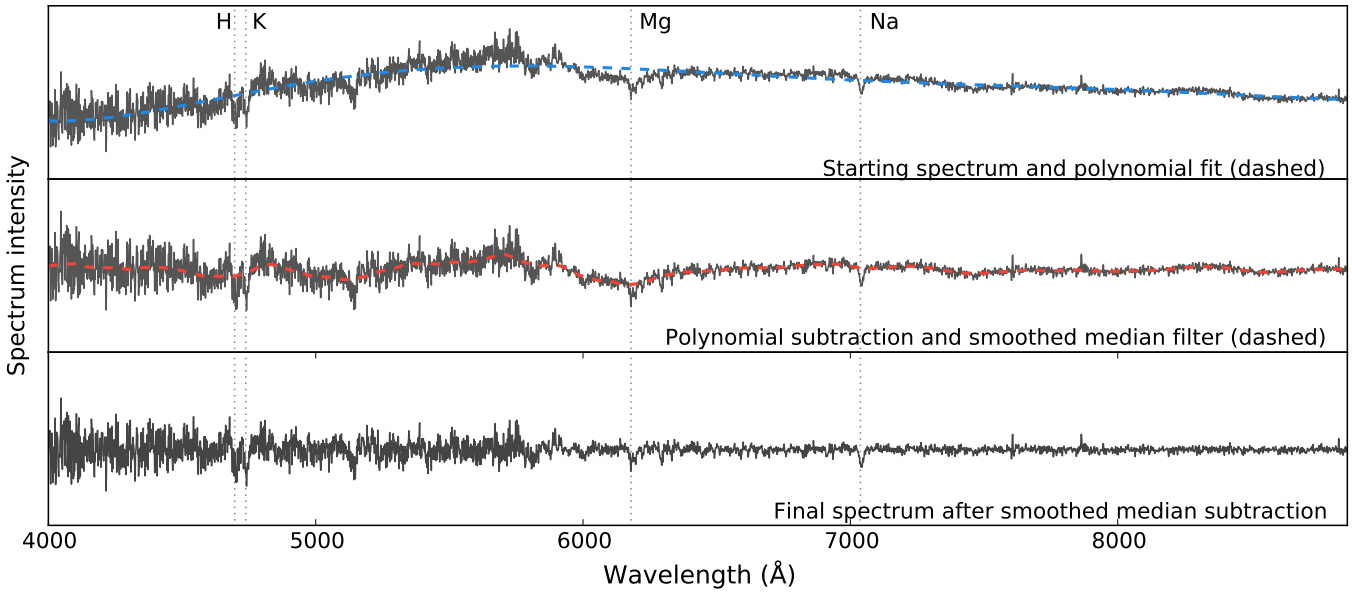

Figure 1. The top subfigure shows an example input spectrum to the continuum removal process. The sixth degree fitted polynomial is shown dashed in this subplot, and the spectrum after subtraction of this polynomial fit is shown in the middle subplot, where we can see that broad continuum features are removed. The middle subplot also shows the output of the smoothed median filtering (dashed), and spectrum after subtraction of this filter is shown in the bottom subplot, where we can see even fine continuum detail has been removed from the spectrum.

at wavelengths close the end of spectroscopic CCD range.

Both the general and the quasar spectrum undergo 60-pixel cosine tapering and root-mean-square normalisation, the former to remove ringing in a Fourier transform and the latter to ensure comparable cross correlation values between different templates. The spectra are oversampled and then Fourier transformed. The quasar spectrum's transformation is then cross correlated with the quasar template, and all other templates are cross correlated with the general spectrum. Cross correlation results are then inverse transformed, with the inverse transformed array representing cross correlation strength over a redshift range. Peaks within allowed redshift ranges for each template are selected, and if prior information on the object type is accessible in the FITS file, the peaks for each template are then weighted. Peaks from all templates are then sorted together, and the ten highest correlation value peaks have a quadratic fit applied around the peak for sub-pixel determination of local maxima. The sub-pixel location of the peaks are converted into a redshift value, and these are returned to the user, with the highest peak representing the best automatic matching found. A potential quality is returned to the user, which is a function of the cross correlation strength of the two greatest peaks, v_1 and v_2 respectively, where the suggested QOP is given by the Eq (2), and the probability of agreement with a human redshifter is illustrated in Figure 3. This suggested QOP is not meant to replace human quality flags, but simply give the redshifter an estimate of spectrum quality before and during manual verification of the automatic result. The suggested QOP is computed from first calculating a Figure of Merit (FOM) from the cross correlation results.

$$\text{fom} = v_1^{0.75} \times \frac{v_1}{v_2} \tag{1}$$

$$QOP = \begin{cases} 6 & \text{if fom} > 4 \text{ and fit to a stellar template} \\ 4 & \text{if fom} > 8 \\ 3 & \text{if fom} > 4 \\ 2 & \text{if fom} > 3.2 \\ 1 & \text{otherwise} \end{cases} \tag{2}$$

4. TEMPLATE SELECTION

It is common in automated matching systems for a large number of templates to be used compared to input spectra. The templates found in MARZ were sourced from original templates from RUNZ, WiggleZ and AutoZ (originally from SDSS). These templates were sorted, compared, and a selection of twelve representative templates were extracted, consisting of five stellar templates, 1 AGN template and 6 galactic templates. Inclusion of a greater number of templates was not found to have a minimal impact on matching performance. Whilst extra target types can be added in the future, there are three challenges for MARZ when attempting to handle a large number of templates. Firstly, users desired to be able to fully replicate the matching capacity of the automatic system when manually redshifting, and a large number of templates complicates the user interface and slows down the process of the user assigning an object type to the spectrum. It would be possible to only display to the user a restricted set of templates, however user feedback indicated this was an undesired solution. Due to the interpreted nature of Javascript and its lack of vector processing capability, computational performance is roughly an order of magnitude worse than on typical compiled code. As the computation time for each spectrum was roughly

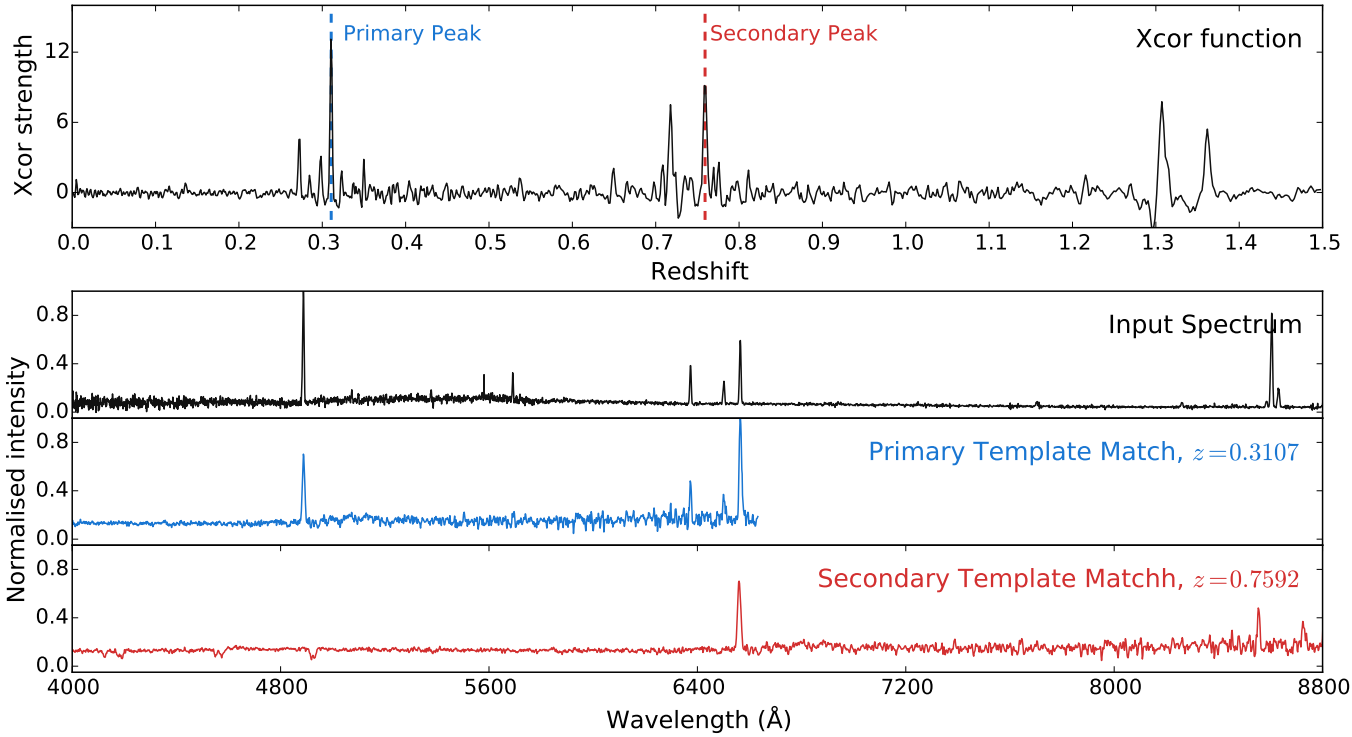

Figure 2. A high quality emission line galaxy spectrum matched against the High Redshift Star Forming Galaxy template. The two strongest cross correlation peaks and the corresponding redshifted template have been displayed beneath the original spectrum for illustrative purposes.

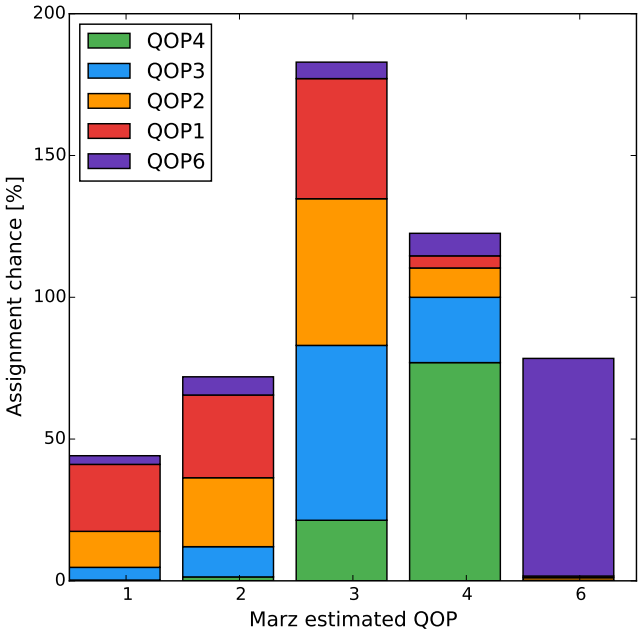

Figure 3. The probability of MARZ assigning a suggested quality differentiated by the quality assigned by a human redshifter. Best performance is in identifying stellar templates by suggesting a QOP of 6, and the amount of low quality (human assigned QOP 1 and 2 spectra) suggested to be good fits by MARZ are primarily due to matching on non-existent features such as improperly subtracted sky lines.

proportional to the number of templates to match, the number of templates was also kept relatively small to ensure that the automatic matching performance was still acceptable on low-end machines. The final concern when adding more templates is the download size of the web application, such that the size of the template dependency remains small enough to be easily redownloaded on page refresh. A potential solution to this is to enable javascript caching of the template file, such that it only needs to be downloaded once.

5. MATCHING PERFORMANCE

Performance testing for MARZ was conducted by looking at two sets of distinct data - one from the OzDES team with low signal-to-noise data at high redshift, and one from the 2dFLenS team with high signal-to-noise data. In both cases, manual redshifting was performed by experienced redshifters in RUNZ, and the automatic matches produced by RUNZ and the automatic results returned by MARZ were compared to the manually assigned redshift for all results assigned a QOP of 4 (99% confidence interval). Comparisons were also made with the AUTOZ program, which is the software being used for the GAMA survey and also being adopted by the 2dFLenS team. These surveys have a smaller number of object types and smaller redshift ranges than OzDES, and therefore have simpler requirements for the redshifting software. These high and low signal-to-noise results are shown in Figures 5 and 6. The redshifting accuracy of MARZ for high signal-to-noise data gave the correct redshift for 97.4% of QOP4 spectra, a failure rate far less than that offered by RUNZ and comparable to AUTOZ. For the low signal-to-noise (high redshift) OzDES data, the accuracy of MARZ was $\approx 92\%$. This is in comparison to the best RUNZ algorithm giving a total accuracy of 54.6%. The lower success rate of AUTOZ, 48.0%, is because the redshift ranges and object types found in the OzDES data are outside the matching

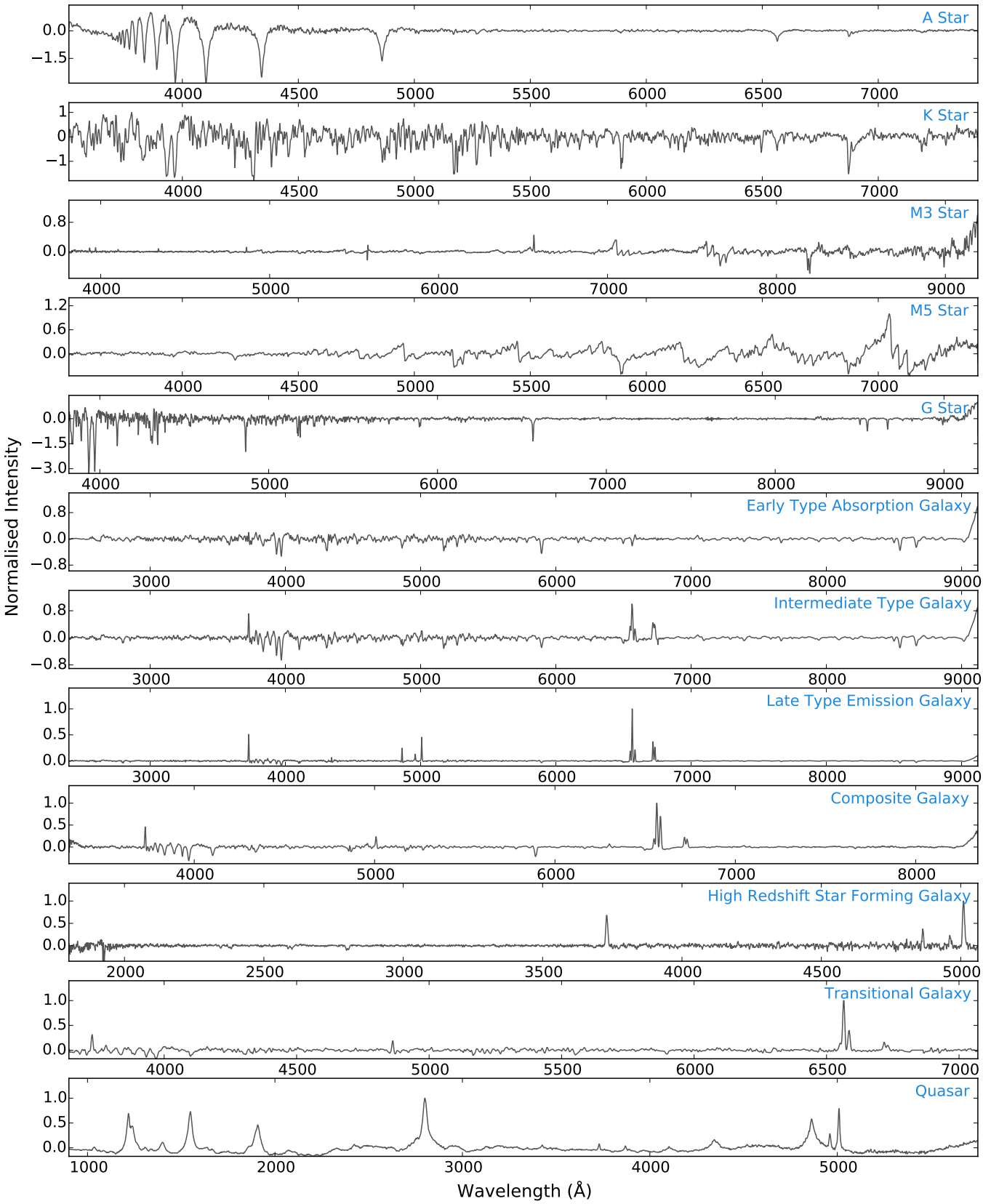

Figure 4. A visual display of the twelve templates in MARZ, displayed after continuum subtraction. The quasar template was created from stitching together multiple templates at different redshifts. The High Redshift Star Forming Galaxy template has been sourced from GDDS Abraham *et al.* (2004)I would like to attribute where each of these come from. Sent email to chrisL and Karl. Waiting on response

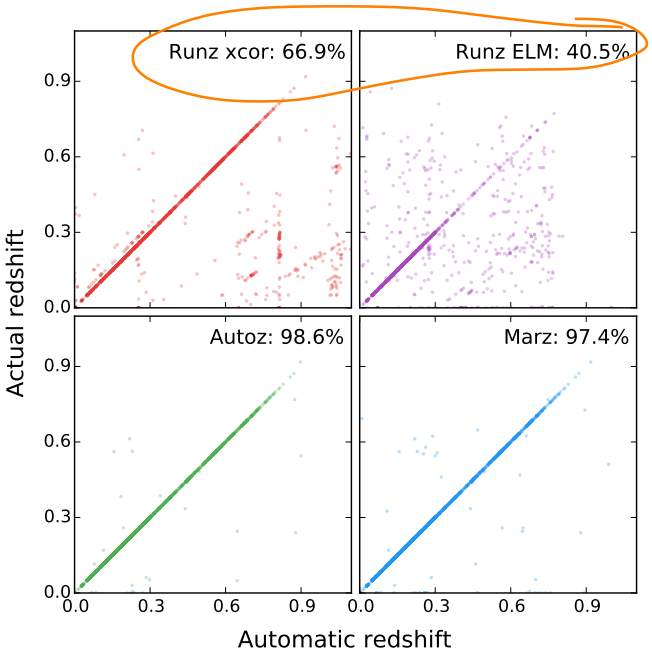

Figure 5. A comparison of matching efficiency using high signal-to-noise data from the 2dFLenS survey and a matching threshold of $\delta z \leq 0.01$. 2217 QOP4 spectra from ten fields are compared in this plot. The vertical axes shows the redshift assigned by an experienced redshifter, and is taken to be correct in this comparison. The horizontal axes show the automatic results of the four algorithms being compared: the RUNZ cross correlation algorithm, the RUNZ emission line matching algorithm, AUTOZ and MARZ. The total accuracy of the algorithms is detailed in the legend. The MARZ algorithm and AUTOZ offer comparable accuracy for high redshift spectra, with AUTOZ pulling ahead slightly due to an increased number of templates being used in the matching process.

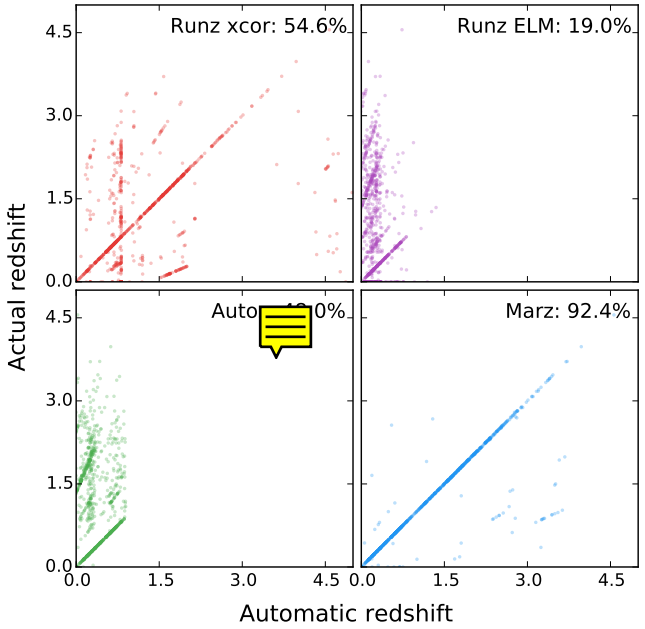

Figure 6. Low signal-to-noise, high-redshift data from the OzDES survey is used in this comparison of matching capability, with a redshift threshold of $\delta z \leq 0.01$. 1083 spectra from eight fields with a redshift range of up to 4.55 are used in this comparison. RUNZ emission line matching performs the worst, with strong diagonal lines of non-unity slope showing repeated spectra feature misidentification. Vertical banding in the RUNZ cross correlation algorithm significantly impacts its effectiveness, and AUTOZ's lack of high redshift templates and hard-coded $z = 0.9$ cutoff make the comparison almost inapplicable. Here the quasar specific matching algorithm used by MARZ stands out, giving a success rate of over 90% for quasar spectra.

capacity of the program.

In addition to the QOP4 successful recovery rates, a normalised probability distribution of likelihood for spectral line misclassification can been produced by combining the high and low signal-to-noise data, where the probability for a misclassification per correct classification can be inspected. This has been done for QOP 4 and QOP 3 (90% confidence) results, in Figure 7. Commonly misidentified spectral lines are labelled in the figure, and can be seen to be a primary source of misclassification across all algorithms. The common $[O_{II}]/[O_{III}]$ misclassification is strongly present in the MARZ failure rates, however its significance drops to approximately 10% of the total failure rate when only QOP4 misclassifications are considered, with the majority of the total failure rate of 4.1% centered around 1. Whilst the expected failure rate for QOP 3 redshifts is ten times higher than for QOP 4 values, this still warrants extra investigation into whether this is a deficiency in the matching algorithm or an effect of the reluctance of human redshifters to assign a QOP 4 quality to spectra matching only on the singular O_{II} feature. If there is an algorithmic deficiency, down weighting of high redshift O_{II} matches could be implemented to reduce the misclassification rate. Commonly misclassified features are also visible on Figure 5 and 6 as linear relationships off the diagonal.

6. INTERACTIVE INTERFACE

The interactive interface consists currently five primary screens: the overview, detailed, templates, settings, and usage screen. The first two screens - the overview and detailed screens, are where users will spend the vast majority of their time, and thus screenshots of them have been provided in Figures 8 and 9. The overview screen provides users with a high level view of the spectra in the loaded FITs file, detailing what they have been matched to and the quality assigned to the matches. Filtering for this screen allows users to sort results or to filter by categories, for example only displaying matches of quality (QOP) 4 or all matches to quasar templates. Comma-separated variable (CSV) output in the form of previously downloaded MARZ results files can be loaded into the program in the same drag-and-drop manner as FITS files, allowing easy verification of redshift results by different users on different machines. A progress bar at the top of the screen keep track of current file completion and file quality.

The detailed screen allows for better verification of automatic matches and also offers the possibility of manually redshifting spectra. Verification of the on screen displayed redshift is done simply by assigning a QOP value, and the top five automatic matches can be cycled if the best match is visibly incorrect. Keyboard shortcuts are available for almost all actions, where key mappings are based off the shortcuts available in RUNZ in order to make transitioning from

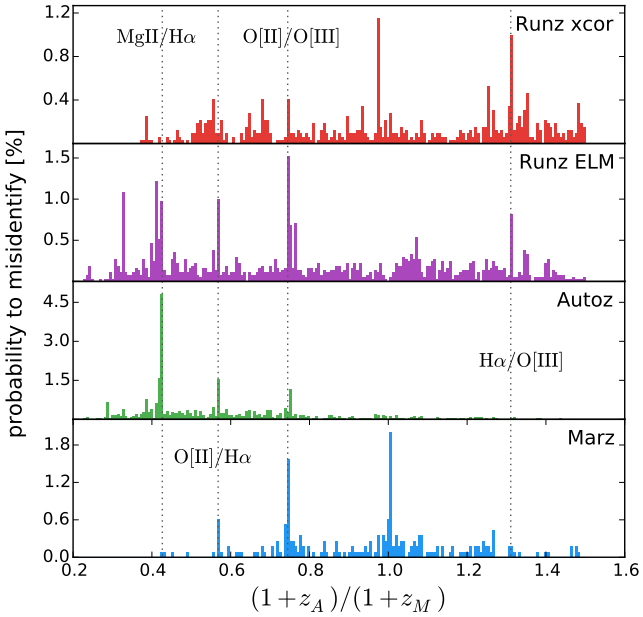

Figure 7. The percentage chance, per successfully assigned redshift of quality 3 or 4, of assigning an incorrect redshift z_A with respect to correct manual redshift z_M. Peaks in the probability distribution generally represent misidentified spectral lines, and common misidentification ratios have had the corresponding spectral lines labelled, such that the first label, MgII/Hα represents the MgII feature misidentified as Hα instead. Performance for RUNZ cross correlation, RUNZ emission line matching, AUTOZ and MARZ are shown respectively in panels (a), (b), (c) and (d). Panel probability axes are not to scale with one another, and the area covered represents the total failure rate. The 2dFLenS and OzDES data from Figures 6 and 5 are combined in this analysis, and QOP3 spectra (90% confidence interval) have been included to give a greater number of sample points. The high relative failure rate of MARZ around $(1 + z_A)/(1 + z_m) = 1$ is due to quasar matching, where the broad features of quasars give a higher uncertainty than well defined emission line spectra. This extra uncertainty in redshift makes it more likely for the manual and automatic redshift to differ by more than the redshift threshold used in the comparison. The total failure rates are given as follows: RUNZ cross correlation: 37.5%, RUNZ emission line matching: 71.0% failure rate, AUTOZ: 18.6% failure rate, MARZ: 6.9% failure rate.

RUNZ to the MARZ as easy as possible. Users can click on features in the detailed plot and then mark them as spectral lines. Matches can be updated by by automatically fitting to the best cross correlation value within a small deviation window. The user can also toggle whether to the display the raw data or the preprocessed data, whether to render a template under the data plot, and whether to display continuum or not. Boxcar smoothing is available to help spectrum legibility.

The templates screen is mostly non-interactive, and simply displays all the templates used by the system with the option to enable or disable specific templates at will. The settings screen gives options to explicitly set how many processing threads to create, whether results should be saved in the background, and offers the ability to clear all saved results in the system, or to simply clear results for the currently loaded FITs. The usage page gives instructions on how to use the program, an explanation of the purpose of each screen, how to raise issues or feature requests via GitHub, and provides several example FITs files for users who simply want to test out the system without having to source a FITs file themselves. It also provides a list of keyboard shortcuts for those users whom are not familiar with RUNZ.

Two main error safeguards have been implemented in the program to stop unnecessary loss of work. The first is a confirmation request when attempting to close down the application, which solves the issue of closing the whole browser with an open tab of MARZ. The second and more robust solution is to use the local storage capacity available in modern browsers to save results in the background after every automatic or manual redshift is assigned. This allows users to close the program, and resume where they left off simply by dragging the original FITS file back into the application.

7. CONCLUSION

Overall, it can be seen that for both high and low signal-to-noise data, MARZ outperforms RUNZ on automatic matching of spectra. MARZ also provides an enhanced and more intuitive user experience, and the web-based nature of the application means that installation and updating are now no longer of any concern at all. As such, MARZ presents a viable alternative to the RUNZ application, and a large step forward in the demonstration of web frameworks as a platform for non-intensive computational analysis. As MARZ simply requires generic FITS files to work, it has redshifting application for other surveys, and can even be used simply to inspect FITS files.

ACKNOWLEDGEMENTS

We would like to thank the OzDES and 2dFLenS teams for their feedback, input and user testing. The MARZ template catalogue comes from the WiggleZ and SDSS template samples, and multiple external libraries have been utilised in the creation of this application: Google's AngularJS, Twitter's Bootstrap, AngularUI, Armit Kapadia's fitsjs, Corban Brook's Digital Signal Processing package, Eli Grey's FileSaver.js, Tom Alexander's regression.js package, lodash and jQuery. Parts of this research were conducted by the Australian Research Council Centre of Excellence for All-sky Astrophysics (CAASTRO), through project number CE110001020.

I have so few references. Need to cite template sources, maybe prior cross cor/matching studies that Ivan references? Should I add in extra figures? Still need to cite 2dflens properly if possible / GAMA maybe (GAMA Im guessing due to autoz? also the authors in the header, don't know what is conventional to put

REFERENCES

Figure 8. The overview screen, showing data from a FITs file courtesy of Chris Blake and the 2dFLenS survey. Users can switch between a sortable tabular view and a graphic tile view, filter on object types, redshift ranges, templates and QOP values. The top of the screen shows the navigation menu, file completion progress bar and input for user initials. Visible at the bottom of the screen is the application footer, which shows the program's progress through automatic matching (automatically matched templates are shown in red in the graphical tiles). The bar changes colour depending on progress - green for preprocessing, red for matching and blue for completed. During the first two stages, a pause button is available to the user. If any results exist, a download button is available, which saves the current results to the file system.

Figure 9. The detailed matching screen, showing spectrum 7 seen in the Overview screen in Figure 8. The menus at the top of the page allow the user to toggle data on or off (variance, sky spectrum, templates and whether to use the raw data or processed data). The menu bar also allows the user to reset to automatic or manual results, smooth the data, select which template to compare against, toggle between the best five automatic results, change the visual offset of the template and manually set the displayed redshift. The user can mark spectral lines by selecting a feature in the plot (either in the main plot or in any callout window) and then select the desired transition (either via keyboard shortcut or by selecting an option in the bottom row of the menu). Users can also change redshift by clicking on peaks in the cross correlation graph found between the spectra plot and the menu bars. Quality values for redshifts can also be assigned via keyboard shortcuts or via the vertical button menu on the left, and assigning a quality saves the result in the background and moves to the next spectrum. In the case where the "QOP 0 only" option is selected in the left hand bar, the user is taken to the next spectrum without a quality flag set, or else it simply takes them to the next spectrum ordered by ID.

F. Yuan, C. Lidman, T. M. Davis, M. Childress, F. B. Abdalla, M. Banerji, E. Buckley-Geer, A. Carnero Rosell, D. Carollo, F. J. Castander, C. B. D'Andrea, H. T. Diehl, C. E. Cunha, R. J. Foley, J. Frieman, K. Glazebrook, J. Gschwend, S. Hinton, S. Jouvel, R. Kessler, A. G. Kim, A. L. King, K. Kuehn, S. Kuhlmann, G. F. Lewis, H. Lin, P. Martini, R. G. McMahon, J. Mould, R. C. Nichol, R. P. Norris, C. R. O'Neill, F. Ostrovski, A. Papadopoulos, D. Parkinson, S. Reed, A. K. Romer, P. J. Rooney, E. Rozo, E. S. Rykoff, M. Sako, R. Scalzo, B. P. Schmidt, D. Scolnic, N. Seymour, R. Sharp, F. Sobreira, M. Sullivan, R. C. Thomas, D. Tucker, S. A. Uddin, R. H. Wechsler, W. Wester, H. Wilcox, B. Zhang, T. Abbott, S. Allam, A. H. Bauer, A. Benoit-Levy, E. Bertin, D. Brooks, D. L. Burke, M. Carrasco Kind, R. Covarrubias, M. Crocce, L. N. da Costa, D. L. DePoy, S. Desai, P. Doel, T. F. Eifler, A. E. Evrard, A. Fausti Neto, B. Flaugher, P. Fosalba, E. Gaztanaga, D. Gerdes, D. Gruen, R. A. Gruendl, K. Honscheid, D. James, N. Kuropatkin, O. Lahav, T. S. Li, M. A. G. Maia, M. Makler, J. Marshall, C. J. Miller, R. Miquel, R. Ogando, A. A. Plazas, A. Roodman, E. Sanchez, V. Scarpine, M. Schubnell, I. Sevilla-Noarbe, R. C. Smith, M. Soares-Santos, E. Suchyta, M. E. C. Swanson, G. Tarle, J. Thaler, and A. R. Walker, ArXiv e-prints (2015), arXiv:1504.03039.

M. Colless, G. Dalton, S. Maddox, W. Sutherland, P. Norberg, S. Cole, J. Bland-Hawthorn, T. Bridges, R. Cannon, C. Collins, W. Couch, N. Cross, K. Deeley, R. De Propris, S. P. Driver, G. Efstathiou, R. S. Ellis, C. S. Frenk, K. Glazebrook, C. Jackson, O. Lahav, I. Lewis, S. Lumsden, D. Madgwick, J. A. Peacock, B. A. Peterson, I. Price, M. Seaborne, and K. Taylor, MNRAS **328**, 1039 (2001), astro-ph/0106498.

W. Saunders, R. Cannon, and W. Sutherland, Anglo-Australian Observatory Epping Newsletter **106**, 16 (2004).

I. Baldry, M. Alpaslan, A. Bauer, J. Bland-Hawthorn, S. Brough, M. Cluver, S. Croom, L. Davies, S. Driver, M. Gunawardhana, *et al.*, Monthly Notices of the Royal Astronomical Society **441**, 2440 (2014).

A. S. Bolton, D. J. Schlegel, É. Aubourg, S. Bailey, V. Bhardwaj, J. R. Brownstein, S. Burles, Y.-M. Chen, K. Dawson, D. J. Eisenstein, J. E. Gunn, G. R. Knapp, C. P. Loomis, R. H. Lupton, C. Maraston, D. Muna, A. D. Myers, M. D. Olmstead, N. Padmanabhan, I. Pâris, W. J. Percival, P. Petitjean, C. M. Rockosi, N. P. Ross, D. P. Schneider, Y. Shu, M. A. Strauss, D. Thomas, C. A. Tremonti, D. A. Wake, B. A. Weaver, and W. M. Wood-Vasey, AJ **144**, 144 (2012), arXiv:1207.7326 [astro-ph.CO].

R. G. Abraham, K. Glazebrook, P. J. McCarthy, D. Crampton, R. Murowinski, I. Jørgensen, K. Roth, I. M. Hook, S. Savaglio, H.-W. Chen, R. O. Marzke, and R. G. Carlberg, AJ **127**, 2455 (2004), astro-ph/0402436